Nonlinear Processes in Geophysics (2000) 7: 159–166

Nonlinear Processes in Geophysics

Numerical simulation of ion dynamics in the magnetotail magnetic turbulence: on collisionless conductivity

A. Greco[1,*], P. Veltri[1*], G. Zimbardo[1,*], A. L. Taktakishvili[2], and L. M. Zelenyi[3]

[1]Dipartimento di Fisica, Università della Calabria, I-87036 Arcavacata di Rende, Italy
2Abastumani Astrophysical Observatory, A. Kazbegi str., 2a, 380060 Tbilisi, Georgia
3Space Research Institute, Profsoyuznaya 84/32, 117810 Moscow, Russia
*Also at Istituto Nazionale di Fisica della Materia, Unità di Cosenza, Italy

Received: 15 November 1999 – Revised: 28 March 2000 – Accepted: 7 June 2000

Abstract. The ion dynamics in the distant Earth's magnetotail is studied in the case that a cross tail electric field and reconnection parity magnetic turbulence are present in the neutral sheet. A test particle simulation is performed for the ions, and moments of the ion distribution function are obtained as a function of the magnetic fluctuation level, $\delta B/B_0$, and of the value of the cross tail electric field, E_y. It is found that magnetic turbulence can split the current carrying region into a double current sheet, in agreement with inferences from observations in the distant magnetotail. The problem of ion conductivity is addressed by varying the value of the cross tail electric field from zero to the observed one: we find that Ohm's law is not enforced, and that a non local, system dependent conductivity is necessary to describe the ion response to the electric field. Also, it appears that the relation between current and electric field may be nonlinear.

1 Introduction

The Earth's magnetotail is a very large and dynamic region of the magnetosphere. Recently, several spacecrafts have shown that a well developed spectrum of low frequency (i.e., below the ion gyrofrequency) magnetic fluctuations is found in the distant tail (Slavin et al., 1985; Hoshino et al., 1994; Nishida et al., 1996; Petrukovic et al., 1999). This turbulence appears to be a permanent feature of the distant tail, and the observed Fourier power density of the turbulent magnetic fields can be approximated by a power law spectrum. In particular, the Geotail magnetic field observations of three-dimensional turbulent magnetic fields may be interpreted as indication of the presence of tearing mode turbulence in the distant tail (Hoshino et al., 1994; Hoshino et al., 1996a; also, Slavin et al., 1985; Nishida et al., 1996).

In order to understand the magnetotail structure and dynamics, it is necessary to study the effects of this magnetic turbulence and of the cross tail electric field on the particle dynamics and on the magnetotail equilibrium structure. The features of a neutral sheet inbedded in a magnetic field reversal with an electric field E_y in the direction of the current were considered by Alfvén (1968) with regard to the magnetopause and the magnetotail current sheets. Because of the drift of electrons and ions in the crossed electric and magnetic fields, the particles move toward the neutral sheet, where the electric field pushes them along the y direction. By applying Ampere's law, Alfvén (1968) obtained the relation $B_0^2/4\pi = en_0L_yE_y$ between the outer value of the magnetic field B_0, the outer number density n_0, the cross tail size L_y and the steady cross tail electric field E_y. We will refer to this configuration as to the Alfvén current sheet. Recently, Veltri et al. (1998) have investigated numerically the influence of magnetic turbulence on the ion dynamics in a magnetic field reversal which represents the Earth's distant magnetotail, and modeled in agreement to the Alfvén current sheet. By using a three-dimensional (3D) magnetic turbulence model, they found that without any scattering agent for the particles one has a current sheet thickness much less than that inferred from the observations (e.g., Pulkkinen, 1996), and a pressure at the center of the neutral sheet which is much too small to enforce pressure balance. On the contrary, the magnetic turbulence is very effective in maintaining the stationary structure of the current sheet and in changing the ion acceleration due to the electric field to thermal motion. In general, the profiles of the current density and of the ion pressure indicate $\delta B/B_0 \simeq 0.3$ as a reasonable value for the level of magnetic fluctuations, in agreement with the observations. Further, Veltri et al. (1998) find that the average time which the ions need to cross the tail in the y direction grows with the fluctuation level $\delta B/B_0$, indicating that the magnetic turbulence can contribute to creating an anomalous resistivity, i.e., a finite collisionless conductivity.

The problem of collisionless conductivity was already considered by Lyons and Speiser (1985), Horton and Tajima (1990, 1991), Horton et al. (1991), and Hernandez et al. (1993), in the case of the middle magnetotail where the normal component B_n of the average magnetic field is not neg-

Correspondence to: G. Zimbardo

ligible and where the field lines have a parabolic shape — the so called quasi-neutral sheet. In that case, it is the mere structure of the average field which produces a chaotic behaviour, and which may mimic a dissipative process. Those authors showed that the collisionless conductivity can be expressed through the particle velocity autocorrelation function, under the assumptions of validity of linearized Vlasov theory, of the fluctuation-dissipation theorem, and of statistically homogeneous system. On the other hand, Holland and Chen (1992) found numerically that a simple proportionality between current and electric field, like in Ohm's law, does not hold because of the existence of trapping in the current sheet. These facts point out the importance of nonlinear dynamics in the magnetotail configurations. A finite collisionless conductivity is of interest for the development of tearing modes, to allow the break down of the frozen in law in the presence of the stabilizing field B_n. Here, however, we are not concerned with the growth of tearing instabilities, but with the effects of the observed magnetic turbulence, which clearly is the result of a non linear process, on particle dynamics. We can envisage the following scenario for the magnetotail neutral sheet at distances between 100 and 200 R_E downtail: due to the smallness of the average magnetic field component normal to the current sheet (Nishida et al., 1994), collisionless dissipation (which is possibly due to microinstabilities at frequencies higher than those considered here) sets in, leading to low frequency tearing turbulence. In turn, this leads to additional dissipation through the effects on particle motion, with enhanced heating and scattering.

In this paper we address the issue of finite collisionless conductivity due to the magnetic turbulence. Indeed, magnetic field reversals with a relevant level of magnetic turbulence are common both in space and in laboratory plasmas. In the case of the distant magnetotail, we adopt the magnetic field model of Veltri et al. (1998), with a turbulence level, typically, of $\delta B/B_0 \simeq 0.3$, and vary E_y from zero to the observed value in order to investigate the dynamical properties of the magnetotail in the case of small electric field. The average electric field E_y is in the range of ± 0.1 mV/m during the quiet times (Nishida et al., 1994) (the geocentric solar magnetospheric (GSM) coordinate system is used in which x is along the Earth-Sun direction, z is oriented in the direction of Earth's magnetic dipole field and y completes the right-handed system). Besides the will to study the current-electric field relation, small values of E_y are motivated by the fact that hybrid numerical simulations of the magnetotail indicate that the electron shielding effectively reduces the electric field in the neutral sheet (Hesse et al., 1996).

In the Sect. 2 we set up the model geometry, the parameters describing the magnetic turbulence, and the simulation code. In Sect. 3 we present the results of the numerical simulation, using several numerical diagnostics to characterize ion conductivity. In Sect. 4 the conclusions are given.

2 Magnetic Field Model and Ion Simulation

In this section we present the main features the magnetic field model of Veltri et al. (1998), which is meant to represent the distant magnetotail. This model consists of a magnetic field reversal and of a 3-D power law spectrum of fluctuations.

In the GSM coordinate system, the average magnetic field $\mathbf{B}^{\rm ave}(z) = B_x^{\rm ave}(z)\mathbf{e}_x$ is in the direction of positive x axis in the upper (northern) lobe and is negative in the lower lobe. It can be chosen as Harris current sheet magnetic field (Harris, 1962), slightly modified in such a way that the asymptotic value B_0 is reached at the edges of the box, where $z = \pm 0.5L$, with zero derivative, $\partial B_x^{\rm ave}/\partial z = 0$:

$$B_x^{\rm ave}(z) = B_0 \frac{\tanh(z/\lambda) - (z/\lambda)\cosh^{-2}(L/2\lambda)}{\tanh(L/2\lambda) - (L/2\lambda)\cosh^{-2}(L/2\lambda)}. \quad (1)$$

Here λ is the current sheet half thickness, and L is the total thickness of the considered magnetic configuration, that is the vertical size of the parallelepipedal simulation box. The observed low frequency magnetic turbulence is modeled as the sum of static magnetic perturbations (Zimbardo et al., 1995; Pommois et al., 1998, 1999):

$$\delta\mathbf{B}(\mathbf{r}) = \sum_{\mathbf{k},\sigma} \delta B(\mathbf{k})\mathbf{e}_\sigma(\mathbf{k}) \exp[i(\mathbf{k}\cdot\mathbf{r} + \phi_{\mathbf{k}}^\sigma)]. \quad (2)$$

Here $\delta B(\mathbf{k})$ is the amplitude of the mode with wave vector $\mathbf{k}$ and polarization σ ($\sigma = 1, 2$), $\mathbf{e}_\sigma(\mathbf{k})$ are the polarization unit vectors, while $\phi_{\mathbf{k}}^\sigma$ are random phases (for more details, see Veltri et al., 1998). As usual, reality of $\delta\mathbf{B}(\mathbf{r})$ implies $\delta B(\mathbf{k}) = \delta B(-\mathbf{k})$ and $\phi_{\mathbf{k}}^\sigma = -\phi_{-\mathbf{k}}^\sigma$. The amplitude is given by the spectrum

$$\delta B(\mathbf{k}) = \frac{C}{(k_x{}^2 l_x{}^2 + k_y{}^2 l_y{}^2 + k_z{}^2 l_z{}^2 + 1)^{\alpha/4+1/2}}, \quad (3)$$

where C is a normalization constant, the spectral index is fixed as $\alpha = 3/2$, which is in the range of values obtained by Hoshino et al. (1994), and l_x, l_y, l_z are the correlation lengths in x, y, and z directions, respectively. Also, L is the scale length in the z direction and RL is the scale length in the x and y directions. In other words, the periodicity of the simulation box is RL, rather than L, in the xy plane, in order to better model the actual magnetotail. In this work, $R \equiv 5$, see Veltri et al. (1998).

The fluctuating component of the magnetic field has been modeled in such a way that it takes into account some features of the tail geometry,

$$l_z \ll l_y, l_x \qquad l_y \approx l_x \quad (4)$$

as well as some characteristics of linear tearing modes. As it is clear from (3), the flat part of the spectrum in each of k_x, k_y, and k_z directions is defined by the corresponding correlation length, and is given by $|k_i| \leq 1/l_i$. The flat part may be considered as the "injection zone" of the spectrum. For $k_i \gg l_i{}^{-1}$, Eq. (3) describes a power law spectrum. We assume that nonlinear interactions between the modes are responsible for the power law part of the spectrum, so that the

larger values of k are the result of an energy cascade (e.g., Malara et al., 1992). On the other hand, the tearing mode growth condition gives the maximum value of k_x in the injection zone as

$$k_x \lambda \leq 1 \tag{5}$$

In order to have a sufficient numerical resolution on the current sheet structure, we fix $\lambda = 0.25L$. Equation (5) then implies $l_x \sim \lambda \sim 0.25L$ and, because of Eq. (4), $l_y \sim 0.25L$. Finally, in our magnetic field model we will use the following values for the correlation lengths:

$$\frac{l_x}{RL} = \frac{l_y}{RL} = \frac{l_z}{L} = 0.05 \tag{6}$$

so that $l_x = 5l_z$, $l_y = 5l_z$. In addition, we impose the tearing parity rules for the perturbed magnetic field on each given mode with wave vector $\mathbf{k}$. These parity rules are the same in the case of the oblique modes which have recently been found by 3D numerical simulation of magnetotail reconnection (Lapenta and Brackbill, 1999). In particular, the x component of the perturbed magnetic field has to have odd parity with respect to the $z = 0$ plane, i.e., $\delta B_x(x, y, z) = -\delta B_x(x, y, -z)$, and the z component of $\delta\mathbf{B}$ has to have even parity, $\delta B_z(x, y, z) = \delta B_z(x, y, -z)$. Taking the sum of the perturbed x and z components with the same k_x, k_y but opposite k_z in Eq. (2) and enforcing the above parity relations, we obtain the following conditions that random phases have to satisfy (Veltri et al., 1998):

$$\phi^1{}_{k_x,k_y,k_z} = \phi^1{}_{k_x,k_y,-k_z} \tag{7}$$

$$\phi^2{}_{k_x,k_y,k_z} = \phi^2{}_{k_x,k_y,-k_z} + \pi \tag{8}$$

The δB_y component has automatically odd parity from these conditions. At the same time, to represent the concentration of the perturbations in the vicinity of the plane $z = 0$ (as observed and as the tearing mode growth indicates, see White et al. (1977)), we will take phases ϕ^1 and ϕ^2 as randomly chosen for the different k_x and k_y but independent of $|k_z|$. In such a case the perturbation amplitude decreases from the center to the boundary, with correlation length given by $l_z = 0.05L$, a feature which has some consequences on the ion dynamics. Vertical profiles of the resulting magnetic perturbation are given in Fig. 1 of Veltri et al. (1998).

2.1 Ion Dynamics Simulation

We will investigate the ion motion in such a turbulent magnetic field, when there is, in addition, a constant electric field in the direction of the unperturbed current. Here, we will restrict our analysis by investigating only ion motion in the current sheet. To first order, ion motion does not depend on the details of the electron dynamics, the latter behaving as a charge neutralizing fluid. Actually, the electrons are magnetized even at $z = 0$ by the assumed magnetic fluctuations, and their response to the cross tail electric field is adiabatic (e.g., Galeev and Zelenyi, 1975; Lembège and Pellat, 1982). Previous numerical simulations have addressed the problem of particle acceleration in magnetic reconnection turbulence, (e.g., Birn and Hesse, 1994). However, we are interested in the features of the current density rather than of particle acceleration.

We assume that the electric field of the tearing perturbations is negligible in the considered cases; this corresponds to the assumption that $v_{thi} \gg V_A$, where v_{thi} is the ion thermal velocity and V_A is the Alfvén velocity. According to our estimates $V_A \leq 200$ km/s, and for particles with energies of 1–2 keV the electric field fluctuations can be neglected. Note that in this case the magnetic field fluctuations can be considered as static, since the ions move much faster than the phase velocity of the waves. In addition, the electric field fluctuations can be effective only on those particles which have the same velocity as the wave phase velocity, which once again requires $v_{thi} \simeq V_A$. Since no resonance condition is required to obtain a significant acceleration by the static field E_y, this will have a much more important effect in accelerating the bulk of particles than the fluctuating field, even when E_y is much smaller than δE.

The equations of motion are

$$m_i \frac{d\mathbf{v}}{dt} = e(\mathbf{E} + \frac{\mathbf{v} \times \mathbf{B}}{c}) \tag{9}$$

where $\mathbf{B} = \mathbf{B}^{\text{ave}}(z) + \delta\mathbf{B}(\mathbf{r})$ and $\mathbf{E} = \mathcal{E}\, E_0 \mathbf{e}_y$, $E_0 = \text{const}$; also, m_i is the ion mass, $\mathbf{v}$ the ion velocity, e the electric charge, and c the velocity of light. We can have equations in a dimensionless form by normalizing all length scales to the box side L, velocities to drift velocity $V_E = cE_0/B_0$, magnetic field to B_0, and time to particle gyrofrequency in B_0, $\Omega_{0i} = eB_0/m_i c$. Note that the magnetic field depends on all of x, y, z, so that no canonical momentum is conserved, and integration is to be carried out in a full six dimensional phase space. A fifth order Runge-Kutta adaptive step integrator is used.

For the distant magnetotail, we have $E_0 = +0.1$ mV/m, and $B_0 = 10$ nT (Nishida et al., 1994; Yamamoto et al., 1994), so that the drift velocity $V_E = cE_0/B_0$ is equal to 10 km/s. Since a reasonable choice for the distant magnetotail current sheet thickness is at least $\lambda = 2500$ km (although larger values were also found, see Pulkkinen et al. (1996)), this implies that $L = 10^4$ km. Ion motion is studied in a 3-D box extending up to 20 L in the cross-tail direction, i.e., from $y = -10L$ to $y = 10L$, up to L in the normal direction, from $z = -0.5L$ to $z = 0.5L$, and up to $5L$ in x. The physical dimension corresponding to the simulation box in the y direction is $L_y = 2 \times 10^5$ km $\simeq 30\, R_E$ and is therefore realistic.

We will use two injection schemes in space. The first injection scheme corresponds to the inflow in the Alfvén sheet, that is particles entering from the planes at $z = \pm 0.5L$, i.e., in principle, from the magnetotail lobes. The values of x and y are chosen at random on the planes $z = \pm 0.5L$. The second injection scheme corresponds to particles entering at $y = -10L$, and at $-0.05L < z < 0.05L$; this scheme is more appropriate to study the single ion velocity correlation function. As far as injection in velocity space is concerned,

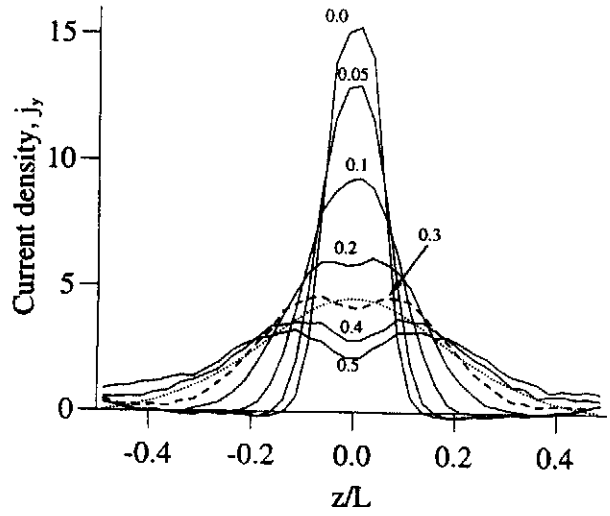

Fig. 1. Current density profiles for $\mathcal{E} = 1$ and various values of the magnetic fluctuation level $\delta B/B_0$. The value of $\delta B/B_0$ is indicated close to each profile. Arbitrary units (Adapted from Veltri et al., 1998).

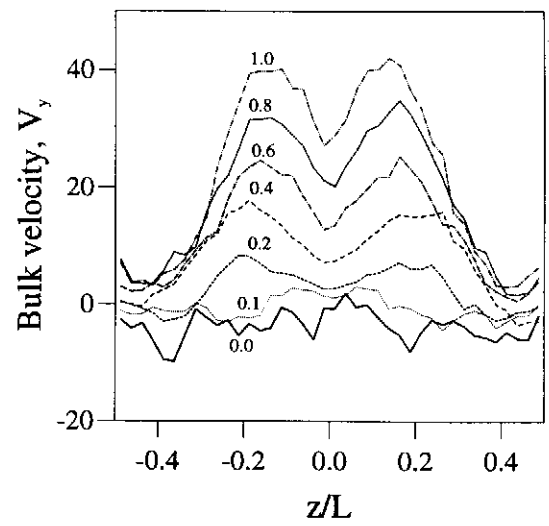

Fig. 2. Bulk velocity profiles for $\delta B/B_0 = 0.3$ and different values of the cross tail electric field $\mathcal{E}$. Velocity in units of V_E (see text). The values of $\mathcal{E}$ are indicated beside each profile.

we assumed a Maxwellian distribution with thermal velocity corresponding to the temperature of 6×10^6 K (Paterson and Frank, 1994). In such a case, $v_{thi} = 22V_E$ at injection. For the first injection scheme, ions are injected in the direction perpendicular to the boundary surfaces with the distribution of the particle flux corresponding to a Maxwellian distribution (see Veltri et al., 1998).

3 Numerical Results

Several runs were made, considering a range of fluctuation levels $\delta B/B_0 = 0.0$–0.5, and values of the dimensionless electric field $\mathcal{E} = 0.0$–1. In the work of Veltri et al. (1998), it was shown that $\delta B/B_0 = 0.3$ is a proper fluctuation level to obtain values for the moments of the ion distribution function, that is density, bulk velocity, current density, temperature, and pressure, which are consistent with those observed in the distant tail by the Geotail spacecraft. When varying $\mathcal{E}$, we will adopt that value for the magnetic fluctuation level. Typically, 2×10^4 particles were injected from the lobes, at $z = \pm 0.5L$.

3.1 Current Density and Velocity Profiles

In a test particle simulation, the current density is defined in arbitrary units, since it is proportional to the number density. We can fix a normalization for the density by requiring that the numerical density at the injection planes, $z = \pm 0.5L$, is exactly equal to what is necessary to maintain the global current in our model. In this way the total current does not depend on $\delta B/B_0$ and on $\mathcal{E}$. In Figure 1 we show the vertical current density profiles for different values of $\delta B/B_0$, and for $\mathcal{E} = 1$, compared to the current profile of the "equilibrium" magnetic field, given by Eq. (2) (dotted line). We note that the current carried by the ions grows in the y direction because of the inflow of particles from the lobes in the Alfvén neutral sheet, and that the total current is constant in y because of the electron current which grows in the opposite direction. Since we are studying only the ion motion, we take all the vertical profiles at the end of the simulation box, $y = 10L$, where the ions represent all of the current. Also, the current profile is averaged in x, which can be considered as a statistically ignorable coordinate, as far as the global structure is concerned. The negative values of j_y found for low $\delta B/B_0$ correspond to the ∇B drift in the negative y direction.

From Figure 1 it is clear that the current profile is very peaked and thin for zero to low fluctuation levels, and becomes progressively broader as the fluctuation level is increased. The fluctuation level which gives a current profile consistent with the average field $B_x^{\text{ave}}(z)$ can be selected by requiring that the current thickness at half-height equals λ. Inspection of Figure 1 shows that the proper fluctuation level is close to $\delta B/B_0 = 0.3$. The same value of $\delta B/B_0$ is obtained by requiring that pressure balance holds across the current sheet (Veltri et al., 1998). On the other hand, another feature emerges from Figure 1: for $\delta B/B_0 \geq 0.2$, the current profile is double peaked, that is the current density is higher at some distance from the neutral sheet than at $z = 0$. The same feature is observed in the profiles of bulk velocity V_y, Figure 2. This means that for sufficient levels of magnetic turbulence, the bulk velocity V_y is small at $z \simeq 0$ because of the concentration of fluctuations near the neutral sheet imposed on our model in Sect. 2. Instead, at some distance from the neutral sheet the magnetic fluctuations are weaker, and ion motion is less disturbed, so that a higher velocity and a higher current density results under the influence of the electric field E_y. Note that such a double humped current profile

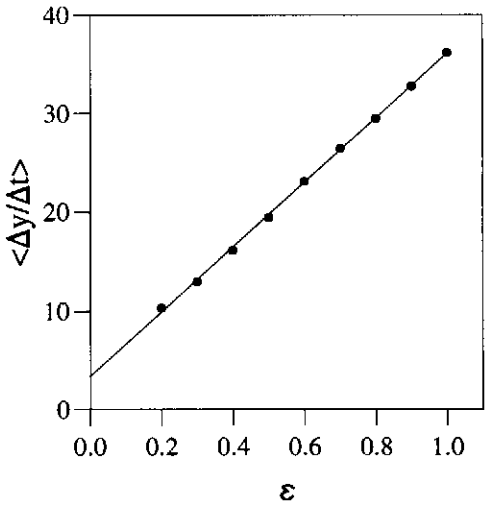

Fig. 3. Current per particle versus $\mathcal{E}$ for $\delta B/B_0 = 0.3$.

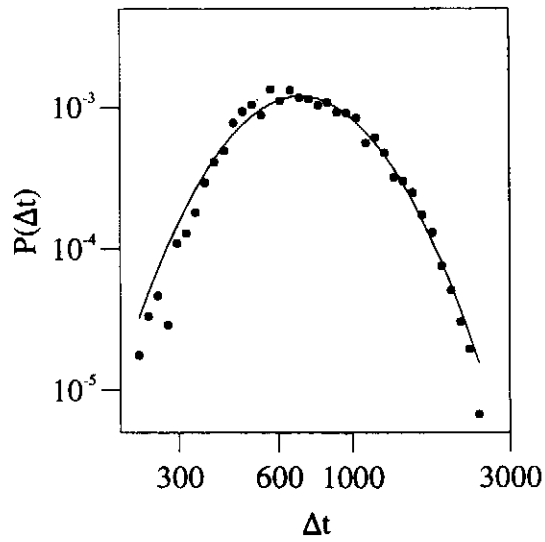

Fig. 4. Probability distribution function $P(\Delta t)$ of the times needed to cross the magnetotail simulation box for $\delta B/B_0 = 0.3$ and $\mathcal{E} = 0.4$. A log-normal distribution (thin solid line) is fitted to the data points.

was inferred from the Geotail observations for the average current sheet by Hoshino et al. (1996b); therefore a strong level of magnetic fluctuations, i.e., $\delta B/B_0 \geq 0.2$ can be an explanation for the observations. A similar effect could be involved in the magnetospheric substorm current disruptions, since the magnetic turbulence level is known to increase during the expansion phase of substorms (e.g., Petrukovich et al., 1999) and a double humped current profile is also inferred (Sergeev et al., 1993). In Figure 2 we plot the bulk velocity V_y versus z for $\delta B/B_0 = 0.3$, and for different values of the electric field $\mathcal{E}$. All the reported velocities are in units of V_E. It is clear that even for small values of the electric field the velocity profile is double humped, and the same is found for the current profiles (not shown). This means that the presence of the double peak is independent of $\mathcal{E}$, and that it is due to the concentration of magnetic turbulence in the center of the neutral sheet. Of course, the bulk velocity decreases with the decrease of $\mathcal{E}$, however we can notice that it is not zero for $\mathcal{E} = 0$. On the contrary, there are several negative peaks, which are due to the ∇B drift in the average magnetic field, and which is in the negative y direction. This is one of the peculiarities of magnetotail magnetic field reversals (e.g., Speiser, 1970; Holland and Chen, 1992; and others).

3.2 Collisionless Ion Conductivity

Veltri et al. (1998) found that the average time needed for ions to cross the simulation box increases steadily with the level of fluctuations $\delta B/B_0$, see Fig. 4 of Veltri et al. This shows that the magnetic turbulence effectively brakes down the ion acceleration due to the electric field, so that this might be a mechanism for collisionless resistivity. As Fig. 2 shows, the bulk velocity increases with $\mathcal{E}$. We can argue that the same would happen for the current density. Following Holland and Chen (1992), we define the current per particle as

$$\langle j_y \rangle = e\langle \frac{\Delta y}{\Delta t} \rangle \tag{10}$$

where Δy is the displacement in y of each ion once the neutral sheet, $z \simeq 0$, has been reached an up to the point when the simulation box is exited, Δt is the corresponding crossing time interval, and the average is made over all particles which exit the simulation box within the maximum allowed time, $t_{\max} = 3000\,\Omega_{0i}^{-1}$. The current per particle is plotted in Fig. 3 versus the electric field for $\mathcal{E} \geq 0.2$. It can be seen that an almost linear relation between $\langle \Delta y/\Delta t \rangle$ and $\mathcal{E}$ is found. However, as indicated by Fig. 2, for smaller values of $\mathcal{E}$ this linear relation is not followed. Also, the best fitting line to the points with $\mathcal{E} \geq 0.2$ does not cross the origin, but has a positive y intercept. Indeed, it is one of the features of magnetic field reversals to induce a net current even in the absence of an applied electric field, for instance because of the ∇B drift and of the Speiser orbits in the neutral sheet (Speiser, 1970; Lyons and Speiser, 1985; Holland and Chen, 1992). Note however that in the case of a strong density concentration in the neutral sheet, like in the Harris sheet, the diamagnetic drift due to the density gradient is stronger than the ∇B drift, and a positive j_y is found at all distances from the neutral sheet. In other words, for $E_y = 0$ the value of the current also depends on the distribution of the plasma, that is on the adopted physical model. Therefore, a relationship of the form $j_y \propto E_y$ cannot be found for all the cases of interest.

In Fig. 4 we show the probability distribution function $P(\Delta t)$ of the above crossing times Δt (computed to obtain

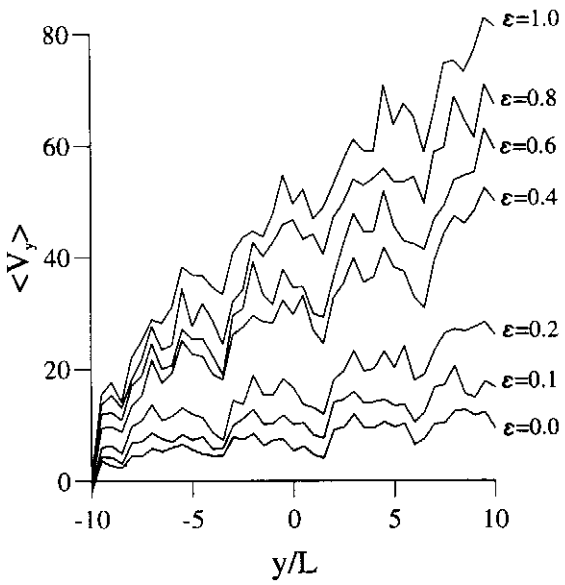

Fig. 5. Bulk velocity V_y at $z \sim 0$ versus y.

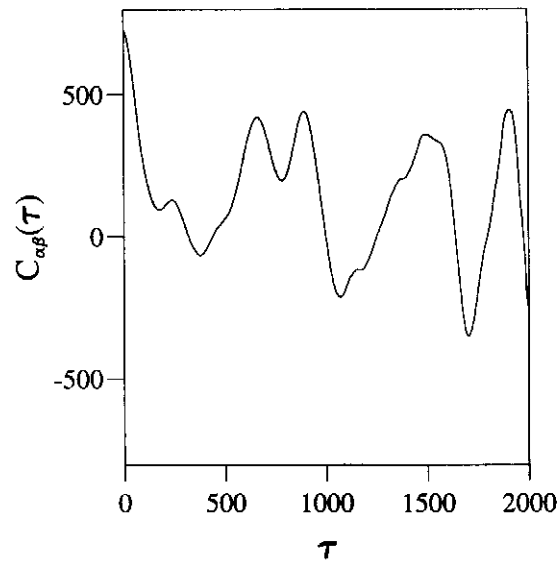

Fig. 6. Velocity correlation function versus time shift τ.

the current per particle) for $\mathcal{E} = 0.4$, in log-log axes. It can be seen that the distribution of crossing times is not Gaussian, but rather it is well fitted by a log-normal distribution. This means that also very long crossing times can be found, and that the story of different particles within the neutral sheet can be very different. Because of the high number of magnetic perturbation modes, we do not have real dynamical traps as in the standard map, but the ion dynamics can be very rich and some ions can be side tracked for very long times. In other words, the magnetic turbulence heavily influences the ion motion, but does not fully replace collisions: in particular, the standard picture of particles being accelerated by E_y and their velocity being randomized by collisions occurring on average after a mean collision time does not hold. In this connection, we plot in Fig. 5 the bulk velocity V_y (measured in the simulation box at $z \simeq 0$ and averaged in x) as a function of y for several values of $\mathcal{E}$: it can be seen that V_y steadily increases with y. Again, this is different from what happens in a Ohmic system, where the current carriers reach a limit velocity (even though it is clear that the magnetic turbulence slows down and thermalizes the ions (Veltri et al., 1998)).

In fact, in a collisionless plasma conductivity can be assessed by kinetic theory rather than by a somewhat ambiguous "collision rate". In order to gain insight into the finite conductivity due to the magnetic fluctuations, we refer to the two time velocity autocorrelation function $C_{\alpha\beta}(\tau)$. Indeed, the conductivity can be expressed as

$$\sigma_{\alpha\beta}(t) = \frac{ne^2}{m_i v_{thi}^2} \int d\mathbf{v}\, f_i(\mathbf{v}) \int_{-\infty}^{t} dt'\, v_\alpha(t) v_\beta(t'), \qquad (11)$$

where $\sigma_{\alpha\beta}(t)$ is the conductivity tensor, n the number density, and f_i the ion velocity distribution function. If it is assumed that the velocity is statistically independent of time translations, one can perform a time average over a period T and obtain (Horton and Tajima, 1990; 1991,; Horton et al., 1991)

$$\sigma_{\alpha\beta} = \frac{ne^2}{m_i v_{thi}^2} \int d\mathbf{v}\, f_i(\mathbf{v}) \int_{0}^{\infty} d\tau\, C_{\alpha\beta}(\tau), \qquad (12)$$

where

$$C_{\alpha\beta}(\tau) = \frac{1}{T} \int_0^T dt\, v_\alpha(t) v_\beta(t-\tau)\,. \qquad (13)$$

In this expression, it is assumed that $C_{\alpha\beta}$ depends only on the time difference τ. The decay of $C_{\alpha\beta}(\tau)$ measures quantitatively the loss of memory of the particles. For a collision dominated plasma, $C_{\alpha\beta}(\tau)$ decays exponentially. In the case of chaotic motion in a parabolic field reversal considered by Horton and Tajima (1991), $C_{\alpha\beta}(\tau)$ decays as a power law, $C_{\alpha\beta}(\tau) \sim \tau^{-m}$, already indicating the presence of long memory effects.

We have computed the ensemble averaged velocity correlation function for the v_y component, $C_{yy}(\tau)$, since this is of main interest for the magnetotail, $j_y = \sigma_{yy} E_y$. For this computation we use the second injection scheme, in the neutral

sheet, to single out the effects of the electric field and of magnetic turbulence when $\mathbf{B}^{ave}$ is small. Fig. 6 shows $C_{yy}(\tau)$ for $\delta B/B_0 = 0.3$ and $\mathcal{E} = 0.4$, averaged over 10^3 particles. In addition, running averages of $C_{yy}(\tau)$ were done, in order to smooth out the variations due to gyromotion. Although a steady decay is found for times up to 200 Ω_{0i}, thereafter C_{yy} has large amplitude oscillations which do not appreciably decay even for very long integration times. This behaviour was consistently found for all the cases with $\mathcal{E} \geq 0.2$. We consider that this is due to the electric field acceleration, which systematically increases v_y. As already indicated by Fig. 5, the fluid velocity also keeps increasing, and the same happens for single particle motion. In such a case the two time velocity correlation function depends on both t and τ, and there is no effective loss of memory. Then $C_{yy}(\tau)$ cannot be used to estimate the conductivity — the time integral in Eq. (15) clearly diverges. Indeed, the validity of Eq. (15) is questionable in our case, both because the long time response to a steady E_y can be outside the range of validity of linear Vlasov theory, and because our system is not homogeneous: to the electric field corresponds a potential energy such that the system is not invariant for spatial translations. Single particle motion is not invariant for time translations, too, because of the energization process. It appears that only a non local (integral) conductivity can account for the magnetotail response to E_y (see Horton et al., 1991). Such an integral conductivity would also depend on the system size, so that a non local, model dependent formulation of the conductivity is necessary. If the regime $\mathcal{E} = 0$ is taken into account, this formulation needs also to be nonlinear.

A further indication of nonlinearity comes from the computation of the ensemble averaged single particle velocity $\langle v_y \rangle$ for a fixed integration time (this differs from the bulk velocity V_y, which is an Eulerian average velocity, whereas $\langle v_y \rangle$ is the average of Lagrangian velocities, with particles at different places). Again using the second injection scheme, we compute $\langle v_y \rangle$ as a function of t for different values of $\mathcal{E}$. In Fig. 7 we plot $\langle v_y \rangle$ versus $\mathcal{E}$, for a set of fixed integration times, in log-log axes: it is evident that $\langle v_y \rangle$ grows almost with the square of $\mathcal{E}$, a very nonlinear behavior. The analysis of these results by means of Lévy random walk models has been undertaken by Zimbardo et al. (2000) and by Greco et al. (in preparation). In order to check whether an asymptotic regime would be reached, such that a saturation of velocity would be obtained, we used very long integration times, up to $t = 6000\ \Omega_{0i}^{-1}$ (this is much longer than the average time which would be needed to cross the magnetotail). Nevertheless, the scaling $\langle v_y \rangle \propto \mathcal{E}^2$ holds at all times, with no indication of saturation. We note that this scaling is totally different from that corresponding to free acceleration, $\langle v_y \rangle \propto \mathcal{E}$, and once more points out the complexity of the influence of magnetic turbulence on the ion motion. Of course, for long integration times the particles overcome the dimensions corresponding to the magnetotail, and may reach such velocities that the streaming instabilities would set in, increasing the effective resistivity of the plasma. However, when staying within the simulation box corresponding to the width of the magnetotail, the ion velocity is much smaller of the thermal velocity (see Veltri et al., 1998), so that streaming instabilities should not grow in the magnetotail. On the other hand, the analysis of such instabilities and of the related resistivity is beyond the scope of this paper.

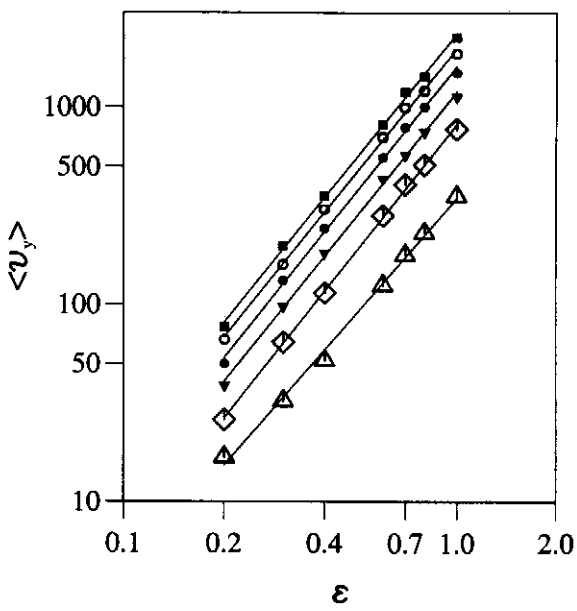

Fig. 7. Average of Lagrangian particle velocity for different integration times, as a function of $\mathcal{E}$, in log-log axes. The integration time, in units of Ω_{0i}^{-1}, is 1000 for empty triangles, 2000 for empty diamonds, 3000 for solid triangles, 4000 for solid circles, 5000 for empty circles, and 6000 for solid squares.

4 Conclusions

From Geotail and other spacecraft observations it appears that low frequency magnetic turbulence is usually present at distances of 100-200 R_E downtail. We can interpret this as a permanent feature of the distant magnetotail, which is easily destabilized with respect to tearing modes due to the negligible value of the normal component of the magnetic field. The resulting turbulence then counteracts the compression due to the cross tail electric field, inflating the current sheet and enabling a quasi-steady equilibrium.

The magnetic turbulence observed by the Geotail spacecraft in the distant magnetotail is reproduced by a numerical model consisting of a modified Harris sheet and a power law magnetic fluctuation spectrum. A test particle simulation is performed in which ions are injected in this magnetic structure and in a constant cross tail electric field E_y. Although the large scale (equilibrium) magnetic configuration is one dimensional, the presence of magnetic turbulence makes the problem fully 3-D. Values of the average cross tail electric field smaller than that observed are also used in order to in-

vestigate the collisionless conductivity, and because an electric field shielding is suggested by the self-consistent numerical simulations (Hesse et al., 1996), too.

The main results are:

1. A splitting of the current density in two sheets is obtained for $\delta B/B_0 \geq 0.2$, in agreement with the current profile deduced from the observations (Hoshino et al., 1996b). The double hump is due to a corresponding increase in the bulk velocity, and this means that the braking due to the magnetic fluctuations is larger in the center of the neutral sheet. The presence of the double hump is not affected by the reduction of the cross tail electric field, unless the latter is very small.

2. The study of the current-electric field relation shows that collisionless conductivity is not easily assessed in our system, in spite of the braking and thermalizing effects of the magnetic turbulence. We find no saturation of V_y, a diverging velocity correlation function, and several indications of a nonlinear relation between the current density j_y and the electric field E_y. It appears that Ohm's law is not satisfied, and that a non local, model dependent formulation of conductivity would be necessary. These results also imply that the meaning of "noise-related" resistivity needs further clarification.

In summary, the considered low frequency magnetic turbulence can enhance ion heating, can influence the current profile by causing it to thicken and to split, and can brake down the electric field acceleration, but this does not correspond to a collisionlike resistivity. On the other hand, a more realistic description of collisionless conductivity in the magnetotail should include the electric fluctuations, time variability, and the electron contribution. We keep these issues for future work.

Acknowledgements. We are grateful to A. V. Milovanov for helpful discussion. This work was financially supported by the Italian MURST, by the Italian CNR, contracts no. 98.00129.CT02 and 98.00148.CT02, by the Agenzia Spaziale Italiana (ASI), contract no. ARS 98-82, and by INTAS Open 97-1612 grant.

References

Alfvén, H., Some properties of magnetospheric neutral surfaces, *J. Geophys. Res., 73*, 4379, 1968.

Birn, J., and M. Hesse, Particle acceleration in the dynamic magnetotail: Orbits in self-consistent three-dimensional MHD fields, *J. Geophys. Res., 99*, 109, 1994.

Galeev, A. A., and L. M. Zelenyi, Tearing instability in plasma configurations, *Sov. Phys. JETP, Engl. Transl., 43*, 1113, 1976.

Harris, E. G., On a plasma sheath separating regions of oppositely directed magnetic fields, *Nuovo Cimento, 23*, 115, 1962.

Hernandez, J., W. Horton, and T. Tajima, Low-frequency mobility response functions for the central plasma sheet with application to tearing modes, *J. Geophys. Res., 98*, 5893, 1993.

Hesse, M., D. Winske, M. M. Kuznetsova, J. Birn, and K. Schindler, Hybrid modeling of the formation of thin current sheets in magnetotail configurations, *J. Geomagn. Geoelectr., 48*, 749, 1996.

Holland, D. L., and J. Chen, On chaotic conductivity in the magnetotail, *Geophys. Res. Lett., 19*, 1231, 1992.

Horton, W., and T. Tajima, Decay of correlations and the collisionless conductivity in the geomagnetic tail, *Geophys. Res. Lett., 17*, 123, 1990.

Horton, W., and T. Tajima, Collisionless conductivity and stochastic heating of the plasma sheet in the geomagnetic tail, *J. Geophys. Res., 96*, 15,811, 1991.

Horton, W., C. Liu, B. Burns, and T. Tajima, Collisionless plasma transport across loop magnetic fields, *Phys. Fluids B, 3*, 2192, 1991.

Hoshino, M., A. Nishida, T. Yamamoto, and S. Kokubun, Turbulent magnetic field in the distant magnetotail: Bot-tom-up process of plasmoid formation?, *Geophys. Res. Lett., 21*, 2935, 1994.

Hoshino, M., T. Mukai, A. Nishida, Y. Saito, T. Yamamoto, and S. Kokubun, Evidence of two active reconnection sites in the distant magnetotail, *J. Geomagn. Geoelectr., 48*, 515, 1996a.

Hoshino, M., T. Yamamoto, T. Mukai, A. Nishida, and S. Kokubun, Structure of plasma sheet current in distant magnetotail: Doubly humped electric current sheet, *Adv. Space Res., 18*(8), 5, 1996b.

Lapenta, G., and J. U. Brackbill, Implicit particle in cell simulation of magnetospheric plasmas, *Geophys. Res. Abstracts, 1*, 668, 1999.

Lembège, B., and R. Pellat, Stability of a thick two-dimensional quasineutral sheet, *Phys. Fluids, 25*, 1995, 1982.

Lyons, L. R., and T. W. Speiser, Ohm's law for a current sheet, *J. Geophys. Res., 90*, 8543, 1985.

Malara F., P. Veltri, and V. Carbone, Competition among nonlinear effects in tearing instability saturation., *Phys. Fluids B, 4*, 3070, 1992.

Nishida, A., T. Mukai, T. Yamamoto, Y. Saito, and S. Kokubun, Magnetic reconnection in geomagnetically active times, 1, Distance to the neutral line, *J. Geomagn. Geoelectr., 48*, 489, 1996.

Nishida, A., T. Yamamoto, K. Tsuruda, H. Hayakawa, A. Matsuoka, S. Kokubun, M. Nakamura, and K. Maczawa, Structure of the neutral sheet in the distant tail ($x = -210$ Re) in geomagnetically quiet times., *Geophys. Res. Lett., 21*, 2951, 1994.

Paterson, W. R., and L. A. Frank, Survey of plasma parameters in Earth's distant magnetotail with the Geotail spacecraft, *Geophys. Res. Lett., 21*, 2971, 1994.

Petrukovich, A.A., L.M. Zelenyi, V. Kudinov, V.N. Lutsenko, A. Milovanov, and G. Zimbardo, Low frequency turbulence in the magnetotail: a noise or an integral part of the tail dynamics?, *Geophys. Res. Abstracts, 1*, 659, 1999.

Pommois, P., G. Zimbardo, and P. Veltri, Magnetic field line transport in three dimensional turbulence: Lévy random walk and spectrum models, *Phys. Plasmas, 5*, 1288, 1998.

Pommois, P., P. Veltri, and G. Zimbardo, Anomalous and Gaussian transport regimes in anisotropic three-dimensional magnetic turbulence, *Phys. Rev. E, 59*, 2244, 1999.

Pulkkinen, T. I., D. N. Baker, C. J. Owen, and J. A. Slavin, A model for the distant tail field: ISEE 3 revisited, *J. Geomagn. Geoelectr., 48*, 455, 1996.

Sergeev, V. A., D. G. Mitchell, C. T. Russell, and D. J. Williams, Structure of the tail plasma/current sheet at $\sim 11\ R_E$ and its changes in the course of a substorm, *J. Geophys. Res., 98*, 17,345, 1993.

Slavin, J. A., E. J. Smith, D. G. Sibeck, D. N. Baker, R. D. Zwickl, and S.-I. Akasofu, An ISEE 3 study of average and substorm conditions in the distant magnetotail, *J. Geophys. Res., 90*, 10,875, 1985.

Speiser, T. W., Conductivity without collisions or noise, *Planet. Space Sci., 18*, 613, 1970.

Veltri, P., G. Zimbardo, A. L. Taktakishvili, and L. M. Zelenyi, Effect of magnetic turbulence on the ion dynamics in the distant magnetotail, *J. Geophys. Res., 103*, 14,897, 1998.

White, R. B., D. A. Monticello, M. N. Rosenbluth, and B. V. Waddell, *Phys. Fluids, 20*, 800, 1977.

Yamamoto, T., K. Shiokawa, and S. Kokubun, Magnetic field structures of the magnetotail as observed by Geotail, *Geophys. Res. Lett., 21*, 2875, 1994.

Zimbardo, G., P. Veltri, G. Basile, and S. Principato, Anomalous diffusion and Lévy random walk of magnetic field lines in three dimensional turbulence, *Phys. Plasmas, 2*, 2653, 1995.

Zimbardo, G., A. Greco, and P. Veltri, Superballistic transport in tearing driven magnetic turbulence, *Phys. Plasmas, 7*, 1071, 2000.